

1 **Supplementary Material: Spectral Phonon Scattering Effects on the Thermal**  
2 **Conductivity of Nano-Grained Barium Titanate**

3 Brian F. Donovan,<sup>1</sup> Brian M. Foley,<sup>1</sup> Jon F. Ihlefeld,<sup>2, a)</sup> Jon-Paul Maria,<sup>3</sup> and  
4 Patrick E. Hopkins<sup>1, b)</sup>

5 <sup>1)</sup>*Department of Mechanical and Aerospace Engineering, University of Virginia,*  
6 *Charlottesville, Virginia 22904, USA*

7 <sup>2)</sup>*Electronic, Optical, and Nanomaterials Department, Sandia National Laboratories,*  
8 *Albuquerque, New Mexico 87185, USA*

9 <sup>3)</sup>*Department of Material Science and Engineering, North Carolina State University,*  
10 *Raleigh, North Carolina 27695, USA*

11 (Dated: 16 July 2014)

---

<sup>a)</sup>Electronic mail: jihlefe@sandia.gov

<sup>b)</sup>Electronic mail: phopkins@virginia.edu

## I. LITERATURE VALUES OF THERMAL CONDUCTIVITY

Particularly in nano-grained and thin film systems, there have been a number of conflicting values reported in the literature for the thermal conductivity of Barium Titanate ( $\text{BaTiO}_3$ ); these are summarized in Table S1. In the mid 1900's, bulk single crystal thermal properties were determined using steady state heat flow techniques by Mante and Volger.<sup>1</sup> More recent measurements of the thermal conductivity of bulk, single crystalline  $\text{BaTiO}_3$  have reported values slightly lower than the original measurements.<sup>2</sup> In 2004, the thermal conductivity of bulk, ceramic  $\text{BaTiO}_3$  was shown to have slightly lower values than the single-crystalline material, most likely due to point defects or grain boundaries introduced by the sintering process.<sup>3</sup>

In terms of the thermal conductivity of polycrystalline/nano-grained  $\text{BaTiO}_3$ , there exists no clear agreement among the reported values in the literature. Jezowski *et al.*<sup>4</sup> measured the thermal conductivity of polycrystalline  $\text{BaTiO}_3$ . The values reported for a ceramic with 100 nm grains were nearly twice the thermal conductivity of bulk single crystal values reported elsewhere. This is also in contrast to values reported by Davitadze *et al.*<sup>5</sup> on 1  $\mu\text{m}$  thin films with roughly 150 nm grains. Jezowski *et al.*<sup>4</sup> also found that for the ceramics with 30 nm grains the thermal conductivity was around  $1.7 \text{ Wm}^{-1}\text{K}^{-1}$ , which is lower than bulk and to be expected with nano-structuring. They explain the wide variation in their data from potential radiation losses and photon thermal conductivity from the surface of their samples due to an optically black ceramic, a characteristic that could also indicate a highly defective material that could result in an increased concentration of electronic carriers as well. Therefore, the measured values reported for their ceramics do not represent the intrinsic phonon thermal conductivity of nano-grained  $\text{BaTiO}_3$ .

## II. FURTHER MATERIALS ANALYSIS

See figures S1 and S2 for additional structure analysis including atomic force microscope images to further show grain size effects as well as X-ray diffraction rocking curves to illustrate epitaxy of the single crystal film.

## III. THERMAL CONDUCTIVITY MEASUREMENT AND MODEL DETAILS

Time domain thermoreflectance (TDTR) utilizes a train of ultra-fast laser pulses to thermally stimulate a material system, and a time delayed probe pulse to measure the change in thermore-

40 flectance due to the decay of the thermal energy deposited by the pump pulse. This work utilizes  
 41 sub picosecond laser pulses emanating from a Ti:Sapph laser system at 80 MHz. The sample is  
 42 irradiated with a train of pump pulses modulated sinusoidally at 8.8 MHz, while the thermoreflec-  
 43 tivity of the time delayed probe pulses are monitored for up to of 6.5 ns after the pump heating  
 44 event on the sample surface. We deposited a nominally 80 nm thin film of Al on the surface of the  
 45 BaTiO<sub>3</sub> to transduce the optical energy from the pulses into thermal energy. The resulting data are  
 46 fit to a model using a least squares method to determine the through-plane thermal conductivity of  
 47 the BaTiO<sub>3</sub> layer given the heat capacity, film thickness, and other layers' thermal properties. We  
 48 assume literature values for the heat capacity of Al (Ref. 6), BaTiO<sub>3</sub> (Ref. 7), and Al<sub>2</sub>O<sub>3</sub> (Ref. 8),  
 49 as well as the thermal conductivity of Al<sub>2</sub>O<sub>3</sub> (Ref. 9). We confirm a more accurate thickness of  
 50  $79 \pm 2$  nm for the Al layer location with picosecond acoustics.<sup>10,11</sup> We assume a reduced thermal  
 51 conductivity of the Al film based on electrical resistivity measurements and the Weidemann-Franz  
 52 law, though we are insensitive to this parameter in our experiment due to our spot sizes and pump-  
 53 probe delay. While we also treat the thermal boundary conductance for the Al/BaTiO<sub>3</sub> interface  
 54 as a free parameter in our model fit, our system is relatively insensitive to this as well as the back-  
 55 side interface conductance. The analysis methods are described in detail elsewhere.<sup>12-14</sup> Reported  
 56 error in the thermal conductivity measurement arises from a combination of small variation of  
 57 thicknesses of constituent materials, particularly in the Al transducer, and measurement of a num-  
 58 ber of different sites on the surface of each sample. Using laser spot sizes of 62.9  $\mu$ m and 13.2  
 59  $\mu$ m diameters for the pump and probe, respectively, allows us to assume that the heating event be-  
 60 ing probed is a fully uniform column, and therefore purely one dimensional in the through-plane  
 61 direction.<sup>12</sup> The measurements over temperature were performed through a transparent window in  
 62 a cryostat cooled by liquid nitrogen.

63 We assume a simple sine-type relation to model the phonon dispersion in our system,<sup>15</sup> which  
 64 has been shown to be a good prediction for mean free path and thermal conductivity elsewhere in  
 65 literature.<sup>16,17</sup> This dispersion model yields a frequency dependence of

$$\omega(k) = \omega_c \sin \left[ \frac{ka}{2} \right] \quad (1)$$

66 We model the group velocity by

$$v_g = v_o \sqrt{1 - \left( \frac{\omega}{\omega_c} \right)^2} \quad (2)$$

67 This leads to a modeled density of states in the form of

$$D(\omega) = \frac{2 \left( \frac{2}{a} \sin^{-1} \left( \frac{\omega}{\omega_c} \right) \right)^2}{\pi \omega_c \sqrt{1 - \left( \frac{\omega}{\omega_c} \right)^2}} \quad (3)$$

68 Using this density of states, phonon velocity, scattering time, and a Bose-Einstein distribution, we  
 69 are able to model thermal conductivity of BaTiO<sub>3</sub> and find fitting parameters to the bulk data given  
 70 as  $A = 700 \times 10^{-17} \text{ s K}^{-1}$ ,  $B = 165 \text{ K}$ , and  $D = 1 \times 10^{-35} \text{ s}^3$ .

71 The model based off of this fitting is included in the figures shown in the main manuscript.

#### 72 IV. DISCUSSION OF GRAY APPROXIMATION

73 For comparison to the spectral model used in this manuscript, we also discuss a gray model<sup>18</sup>  
 74 in which there is a single mean free path of the phonons in a system at any given temperature. To  
 75 determine the values of this gray mean free path, we turn to literature values for heat capacity and  
 76 thermal conductivity and rearrange the equation

$$\kappa = \frac{1}{3} C v \lambda \quad (4)$$

77 to

$$\lambda_{gray}(T) = \frac{\kappa(T)}{\frac{1}{3} C(T) v} \quad (5)$$

78 This enables us to use temperature dependent literature values for thermal conductivity,  $\kappa$ , and heat  
 79 capacity,  $C$ , along with the speed of sound,  $v$ , to determine the gray mean free path of phonons in  
 80 bulk BaTiO<sub>3</sub> as a function of temperature. By this process we determine that, at room temperature,  
 81 the gray model predicts a phonon mean free path in bulk BaTiO<sub>3</sub> of  $\lambda_{bulk} = 2.3 \text{ nm}$ . This result  
 82 in itself would suggest that introducing grain-boundaries from 36 - 63 nm grains should have no  
 83 effect on the thermal conductivity in the system, which is very clearly not the case. To further  
 84 illustrate this, and validate the spectral model of thermal conductivity in this system, we turn to  
 85 a comparison of models over temperature. Using the same approach to formulate scattering time  
 86 as discussed in the manuscript, we determine the total scattering predicted by the gray model by  
 87 Matthiessen's rule.

$$\frac{1}{\tau} = v \left( \frac{1}{\lambda_{gray}} + \frac{1}{d_{film}} + \frac{1}{d_{gb}} \right) \quad (6)$$

88 The resulting prediction for thermal conductivity of the thin film, nano-grained system, with  
 89 36 nm grains as an example, are shown in Fig. S3. We see that this prediction does not accurately  
 90 depict the data measured, showing only a very small deviation from bulk thermal conductivity at  
 91 operating temperatures. The trend given by the gray model also helps to illustrate the quality of fit  
 92 of the simple spectral model included in the manuscript to the data measured.

## 93 REFERENCES

- 94 <sup>1</sup>A. Mante and J. Volger, *Physics Letters A* **24**, 139 (1967).
- 95 <sup>2</sup>M. Tachibana, T. Kolodiaznyy, and E. Takayama-Muromachi, *Applied Physics Letters* **93**,  
 96 092902 (2008).
- 97 <sup>3</sup>Y. He, *Thermochimica Acta* **419**, 135 (2004).
- 98 <sup>4</sup>A. Jezowski, J. Mucha, R. Pazik, and W. Strek, *Applied Physics Letters* **90**, 114104 (2007).
- 99 <sup>5</sup>S. T. Davitadze, S. N. Kravchun, B. A. Strukov, B. M. Goltzman, V. V. Lemanov, and S. G.  
 100 Shulman, *Applied Physics Letters* **80**, 1631 (2002).
- 101 <sup>6</sup>G. Furukawa, M. Reilly, and J. Gallagher, *Journal of Physical and Chemical Reference Data* **3**  
 102 (1974).
- 103 <sup>7</sup>S. S. Todd and R. E. Lorenson, *Journal of the American Chemical Society* **74**, 2043 (1952).
- 104 <sup>8</sup>D. A. Ditmars, S. Ishihara, S. S. Chang, and G. Bernstein, *Journal of Research of the National*  
 105 *Bureau of Standards* **87**, 159 (1982).
- 106 <sup>9</sup>V. Pishchik, L. A. Lytvynov, and E. R. Dobrovinskaya, *Sapphire - Material, Manufacturing,*  
 107 *Applications, Micro- and Opto-Electronic Materials, Structures, and Systems* (ISBN 978-0-387-  
 108 85695-7, 2009).
- 109 <sup>10</sup>C. Thomsen, J. Strait, Z. Vardeny, H. J. Maris, J. Tauc, and J. J. Hauser, *Phys. Rev. Lett.* **53**, 989  
 110 (1984).
- 111 <sup>11</sup>C. Thomsen, H. T. Grahn, H. J. Maris, and J. Tauc, *Phys. Rev. B* **34**, 4129 (1986).
- 112 <sup>12</sup>P. E. Hopkins, J. R. Serrano, L. M. Phinney, S. P. Kearney, T. W. Grasser, and C. T. Harris,  
 113 *Journal of Heat Transfer* **132**, 081302 (2010).
- 114 <sup>13</sup>D. G. Cahill, *Review of Scientific Instruments* **75**, 5119 (2004).
- 115 <sup>14</sup>A. J. Schmidt, X. Chen, and G. Chen, *Review of Scientific Instruments* **79**, 114902 (2008).

- <sup>116</sup> <sup>15</sup>C. Kittel and P. McEuen, *Introduction to solid state physics*, Vol. 8 (Wiley New York, 1986).
- <sup>117</sup> <sup>16</sup>R. Yang and G. Chen, *Phys. Rev. B* **69**, 195316 (2004).
- <sup>118</sup> <sup>17</sup>P. E. Hopkins, P. M. Norris, and J. C. Duda, *Journal of Heat Transfer* **133**, 062401 (2011).
- <sup>119</sup> <sup>18</sup>G. Chen, *Phys. Rev. B* **57**, 14958 (1998).

TABLE S1. Various literature values of thermal conductivity ( $\kappa$ ) for bulk & nano-structured BaTiO<sub>3</sub> at Room Temperature

Data Source (year)	Avg. $\kappa$ of BaTiO <sub>3</sub> @ RT (Wm <sup>-1</sup> K <sup>-1</sup> )	Sample Type	Measurement Method
Mante & Volger <i>Physica</i> (1967)	5.7	Bulk Single Crystal	Steady State Heat Flow
Tachibana <i>et al. APL</i> (2008)	3.4	Bulk Single Crystal	Bulk Meas System
He <i>et al. Therm Acta</i> (2004)	2.7	Bulk Ceramic	Hot Disc
Davitadze <i>et al. APL</i> (2002)	5.1	1 $\mu$ m Thin Film w/ 150nm Grains	3 $\omega$ method
Jezowski <i>et al. APL</i> (2007)	10.22	Bulk Ceramic w/ 100nm Grains	Axial Stationary Flow
Jezowski <i>et al. APL</i> (2007)	1.73	Bulk Ceramic w/ 30nm Grains	Axial Stationary Flow
This Work	2.17 $\pm$ 0.22	175 nm Epitaxial Thin Film	TDTR
	1.71 $\pm$ 0.06	175 nm Thin Film w/ 63nm Grain	TDTR
	1.42 $\pm$ 0.07	175 nm Thin Film w/ 52nm Grain	TDTR
	1.27 $\pm$ 0.1	175 nm Thin Film w/ 47nm Grain	TDTR
	1.08 $\pm$ 0.07	175 nm Thin Film w/ 42nm Grain	TDTR
	1.00 $\pm$ 0.09	175 nm Thin Film w/ 36nm Grain	TDTR

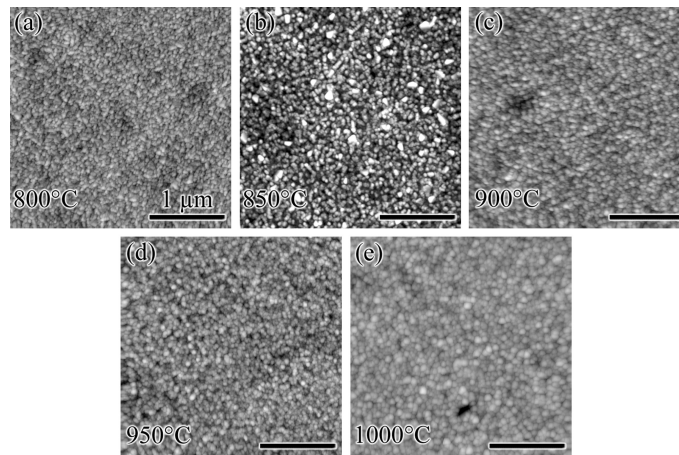


FIG. S1. 3  $\mu$ m x 3  $\mu$ m contact mode topographic atomic force microscope images of polycrystalline BaTiO<sub>3</sub> films annealed at (a) 800°C, (b) 850°C, (c) 900°C, (d) 950°C, and (e) 1000°C.

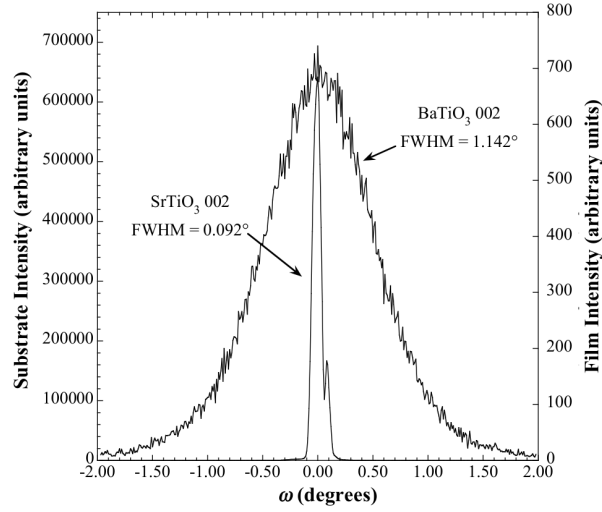


FIG. S2. X-ray diffraction rocking curves of the substrate and film 002 reflections. Full width at half maximum (FWHM) values for the substrate and film are  $0.092^\circ$  and  $1.142^\circ$ , respectively.

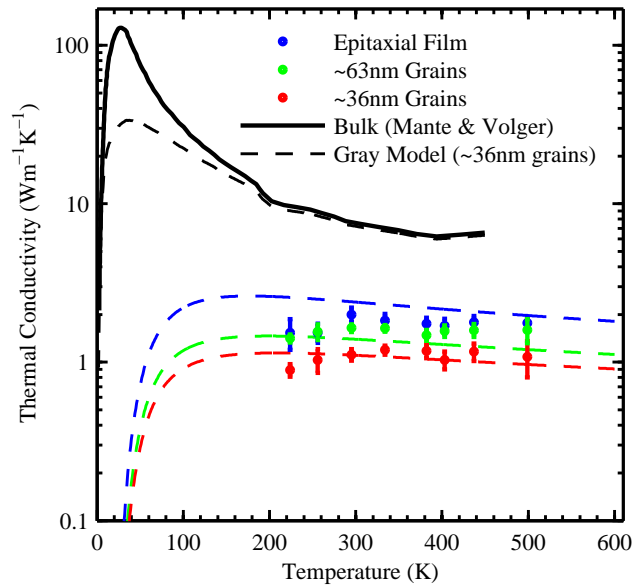


FIG. S3. Thermal conductivity of BaTiO<sub>3</sub> over varying sample temperature for two nano-grained and a single crystal thin film with respective modeled trends. Included is the prediction by the gray for the 36 nm grain, thin film samples, showing very little deviation from bulk values<sup>1</sup> when neglecting the spectral nature of the phonons in the system.